# Ex-situ up-conversion of biomass pyrolysis bio-oil vapors using $Pt/Al_2O_3$ nanostructured catalyst synergistically heated with steel balls via induction

Mohammad Abu-Laban[1], Pranjali D. Muley[1], Daniel J. Hayes[1], and Dorin Boldor[1,*]

[1]Department of Biological & Agricultural Engineering, Louisiana State University Agricultural Center and A&M College, Baton Rouge, Louisiana 70803, United States of America

[*]Corresponding author. Email address: dboldor@agcenter.lsu.edu

ABSTRACT

Radiofrequency-driven hydrodeoxygenation of sawdust pyrolysis vapor and the coking performance of the catalysts were investigated using $Pt/Al_2O_3$ commercial pellets mixed with steel balls inside an alumina tube. The radio-frequency induction heating of the catalyst bed was compared with a conventional method of heating using electric tape engulfing the catalyst bed reactor. Partial deoxygenation of the oil was successfully achieved in the catalytic upgrading of pyrolysis oil at 234°C, with the use of the induction heater. The molar O/C ratio of the oil decreased from 1.36 to 0.51. No deoxygenation of the oil was observed using the electric tape control under identical conditions as both carbon and oxygen appeared to be removed at approximately equal rates, with the carbon being deposited in the form of coke onto the catalyst instead of being recovered in the liquid.

KEYWORDS

Induction Heating

Hydrodeoxygenation

Pyrolysis

Coking

Steel balls

## 1. Introduction

Research into biofuels as an alternative energy source to crude oil has drawn much attention and success was achieved for the up-conversion of bio-oil derived from lignocellulosic biomass with the use of catalytic hydrodeoxygenation (HDO) [1-4]. One of the most widely used methods for the thermochemical decomposition of pine sawdust to produce bio-oil is fast pyrolysis, in the absence of oxygen. Raw bio-oil possesses a relatively small heating value, due mainly to its highly oxygenated organic, mostly phenolic, compounds that make up a significant amount of its chemical composition. Water composition of the liquid product from pine pyrolysis is reported at an average 17% by weight, while average oxygen content of the organic phase is reported at 47 wt. % [5]. The higher heating value (HHV) of wood pyrolysis oil averages around 16-19MJ/kg compared to heavy fuel derived from petroleum which is reported at 40MJ/kg [6]. In addition to low calorific values, the high oxygen content makes the bio-oil non-ideal for storage due to its reactivity. This volatility in the chemical makeup of the pyrolysis bio-oil renders its utilization as a chemical feedstock difficult due to the variability in the physical and chemical properties.

As mentioned above, up-conversion of the bio-oil to reduce oxygen content and respectively to increase the energy density and quality of the bio-oil can be achieved via catalytic deoxygenation. In this process, through a series of hydrogenation, deoxygenation and dehydration reactions, the carbonyl groups are hydrolyzed and removed to produce water and reduce the oxygen content in the organic oil phase. In the study reported in [4], m-cresol was used as a bio-oil model compound to study its deoxygenation over Pt/γ-$Al_2O_3$ catalysts under low pressure hydrogen gas. The main products of the hydro deoxygenation reaction were

reported to be toluene, benzene and methylcyclohexane. While high pressure hydrogen is also used in the HDO processes for coke removal [2, 7], the high amount of hydrogen unutilized makes a low-pressure hydrogen source more desirable. Selection of Pt in the proposed study as the most selective reducing metal toward benzene formation, as well as of low-pressure hydrogen were thus based on existing literature data [8-13].

In [3], the catalytic deoxygenation of pyrolysis oil derived from *Leucaena leu-cocephala* and other wood species, including pine sawdust, was also studied using $Pt/Al_2O_3$ catalysts. The study reports a decrease in the molar O/C ratio from 0.4 to 0.16 after deoxygenation. In the reported case, the liquid oil was first generated and then mixed with the catalyst in a heated continuous stirred-tank reactor (CSTR), whereas in the study reported here, the catalysis occurred ex-situ immediately after the pyrolysis reaction, while the bio-oil was still in vapor form.

In the proposed study we look at a unique method of heating the catalyst using radiofrequency inductive heating, a method also applied to the biomass pyrolysis process, as discussed in previous reports [14, 15]. With the insight gained from these reports into optimal reactor residence times, biomass pyrolysis temperature and yields, the current study builds on that information to upgrade the quality of the oil by passing the vapors through a catalyst bed composed of a steel-$Pt/Al_2O_3$-mix for hydrodeoxygenation, as opposed to a regular HZSM-5 as reported in [15] ([14] did not report any upgrading of the produced bio-oil). In this work, inductive heating of the steel balls was employed to maintain the bed temperature in an electrically non-conductive alumina reactor, whereas the work reported in [15] used a steel reactor, which indirectly heats the catalyst. Direct heating of the mixture of catalyst and a

metallic susceptor using RF-based induction ensures that the catalyst acts as a heat source as opposed to heat sink observed for conventional heating techniques, and discourages the cooling and condensation of pyrolysis vapors on the surface of the catalyst and subsequent coke formation. This opens the door for the development of catalyst particles seeded onto RF-receptive materials such as iron that can be heated directly by radiofrequency waves to increase the temperature of the catalyst bed, reversing the flow of heat from exterior-to-interior to interior-to-exterior.

The principle of an induction heater is well established, and involves an alternating current passing through a coil which induces an alternating magnetic field within the volume enveloped by the coil. The alternating magnetic field in turn induces eddy currents on any electrically-conductive load placed in the same volume [16]. Benefits of the induction heating include the efficient and rapid heating of the load, since the only heat being generated originates from the load itself with very little to no heat loss to the surrounding. More importantly, the positive temperature gradient established across the catalyst surface would ideally deter the polycondensation and polymerization of the vapor molecules, preventing tar and coke formation.

In the proposed study, we look, for the first time to our knowledge, at the heating profiles under different powers for the catalyst bed using stainless steel balls mixed with HDO pellets within a *non-conductive tube* using this type of electromagnetic heating. The non-conductive tube does not interact with the induction field, and thus does not contribute to the heating process. Only the steel balls and, to a much smaller extent, the $Pt/Al_2O_3$ pellets are heated directly by the electromagnetic field. Components in pyrolysis oil can begin to condense

at temperatures below 300˚C [17], depending on the originating biomass and the organic compounds resulting from the specific pyrolysis process. Therefore, in general, it is necessary to maintain the bed temperature to avoid cooling of the pyrolysis vapors coming from the biomass reactor. In addition, it is also desirable to set the temperature close to, or at, the point at which optimal reducing activity of the catalyst occurs, based on their temperature-programmed reduction and desorption profiles. The hydrogen TPR and ammonia TPD results indicate the temperature regions at which the sites are most reactive to hydrogen adsorption, and acid sites are weak and more reactive in the bonding of oxygenated compounds. These temperature regions would be the conditions ideal for the hydrodeoxygenation pathway.

While several studies have looked at the mitigation of coke formation [18-20], there is little understanding of the effect of the surface catalyst temperature and the role it plays in the adsorption of coke molecules. Generally, adsorption is exothermic and an increase in temperature leads to a decrease in adsorption. However, the condensation of molecules on the surfaces can also be due to the temperature gradient across the surface of the catalyst. A negative temperature gradient can lead to a faster rate of the coke adsorption. Hence, the heating method of the catalyst reactor can play a significant role in the formation of fouling compounds on the surface sites that reduce the catalysts longevity. By using the novel method of inductive heating of the steel bed, it is hypothesized that by directly heating the catalyst from the interior of the bed, the rate of condensation of the oil vapors and coke formation on the catalytic sites can be significantly reduced, relative to a conventional heating method. As a result, it is expected that the oxygen content of the collected oil is reduced for the inductive

method as the catalyst performance endures and the carbon content is maintained in the vapor flow.

## 2. Materials and Methods

### *2.1 Materials*

3.2mm Pt (1wt. %) /$Al_2O_3$ pellets and 99% dichloromethane (DCM) were purchased from Sigma-Aldrich®, one 5% $H_2$/balance $N_2$ gas cylinder (200$ft^3$) was purchased from AirLiquide and Type 316 stainless steel precision balls, 7/32" diameter, were purchased from McMaster-Carr. A custom-made alumina ceramic tube was ordered from SentroTech. Pine shavings from scrap wood (untreated) were collected from the in-house wood shop in the Biological and Agricultural Engineering Department at Louisiana State University Agricultural Center (LSU AgCenter).

### *2.2 Catalyst Characterization*

The Pt/$Al_2O_3$ pellets were tested as received for Temperature-Programmed Reduction, Desorption (TPR, TPD) and BET analysis. All analyses were performed using an Altamira 200R-HP unit with the catalyst placed inside a 1/4" ID u-shaped quartz tube. Products were analyzed with a thermal conductivity detector (TCD).

#### *2.2.1 Temperature Programmed Reduction [4]*

For pre-treatment, Helium gas was flushed through at 30cc/min. The temperature was ramped to 150˚C at 10˚C/min and held for 30 minutes, and then cooled to 40˚C at 10˚C/min. The TPR treatment followed with the use of 10% $H_2$/Ar gas at 30cc/min, and ramped to 900˚C at 10˚C/min.

#### *2.2.2 Temperature Programmed Desorption [3]*

The pellets were first pre-treated with Helium gas flushed at 30cc/min, heated to 250˚C at 10˚C/min and held for 60 minutes. The bed was then cooled to 100˚C at the same rate. To adsorb $NH_3$, 10% $NH_3$/He was injected at 30cc/min for 10 minutes. This was followed by flushing again with He gas to desorb the ammonia, at 30cc/min and temperature ramping to 900˚C at 10˚C/min.

*2.2.3 BET*

A 3-point Brunauer-Emmett-Teller analysis was performed according to literature [21]. The catalyst was first pre-treated with He gas, with temperature increased to 150˚C at 10˚C/min and held for 30min. The quartz tube was then cooled to 40˚C at the same rate. The catalyst was then outgassed with pure nitrogen at 50cc/min. Data was collected over three pulse periods during which the bed was submerged in liquid nitrogen three times for 300s long each.

*2.3 Biomass Pyrolysis Setup*

The experimental parameters for the pyrolysis of sawdust were previously developed [14, 15]. Pine sawdust shavings were ground and filtered to <0.5mm in diameter and dried overnight. The feed-to-catalyst ratio was set after initially using a high ratio that was subsequently reduced in preliminary experiments until significant production of benzene and reduction of phenolic compounds was observed from the GC-MS spectra of the oil phase [14, 15, 22]. Based on these preliminary data, 10g of the treated sawdust was packed into the center of an insulated 310-stainless steel tubular reactor. This biomass reactor was suspended within an RF induction coil (10-loop, rubber-insulated copper coil, 285mm in length and 59mm ID), connected to a low frequency induction heater (RDO Inc., model LFI 35-100kHz). The biomass reactor was connected to a 5%$H_2$/bal. $N_2$ gas line, and to the catalyst bed in series. The

catalyst bed consisted of 25g of 1wt. % Pt on $Al_2O_3$ pellets inside a 1.25”OD X 0.70”ID, 10” long 99.8% alumina tube with low magnetic permittivity. The pellets were mixed with 400g of 7/32" diameter stainless steel balls to full capacity of the tube in order to increase the load for inductive heating. The catalyst bed was under its own induction heater (6-loop coil, rubber insulated, 203mm in length and 49mm ID, RDO, Inc. model HFI 135-400kHz). The system was purged with 5% hydrogen gas flowing at 3 CFH for 1h prior to the biomass pyrolysis. During this flushing time, the catalyst bed was heated to the desired target temperature and maintained for one hour to reduce any oxidized Pt prior to initiating pyrolysis. This temperature was maintained throughout each individual experiment. Vapors from the biomass reactor passed through the catalyst bed and entered a condensation flask submerged in ice which was connected to an electrostatic precipitator, as described in [15]. The exit stream from the condenser lead to ethanol and water traps, connected serially to collect any soluble compounds, and then to the outlet stream. Gas samples were collected at the junction prior to the water and ethanol traps and analyzed with gas chromatography.

An infrared sensor coupled to an Omega iR2C PID controller (OMEGA Engineering, Inc., Stamford, CT) was used to control the temperature of the biomass reactor at 550˚C by adjusting the power output of the LFI induction heater. The temperature of the catalyst bed tube was manipulated manually by setting the power level to one value and allowing the surface temperature of the tube to reach a maximum steady state value. This adjustment was performed for 3 different power levels (250W, 350W, and 500W) to achieve 3 different bed temperatures (234°C, 286°C, and 375°C). The surface temperature of the alumina tube was monitored and recorded in real time using an IR camera (FLIR A325sc, FLIR Systems, Inc.,

Wilsonville, OR) connected to thermal data acquisition software (ThermaCAM Professional 9.1, FLIR Systems, Inc., Wilsonville, OR). The temperature readings at four different points along the length of the tube were recorded and averaged to obtain the tube surface temperature (Figure 1). The emissivity value of the alumina tube was set to 0.9 and confirmed via trial and error using a thermocouple.

To compare the inductive heating method to a conventional heating source, an electrical heating tape was used as our control experiment. The electrical tape operated with an on-off feedback controller. The temperature set point was set equal to the induction-heated run at the temperature in which the optimal results, based on the O/C and HHV values of the oil product, were attained. In addition, a baseline experiment was set up and tested in which the pyrolysis of sawdust was carried out under identical conditions, but without any catalytic up-conversion. All experiments were performed in duplicates.

Based on the parameters reported [14, 15], pyrolysis of the sawdust proceeded for 20-25min for optimum reaction time, which was the time necessary for the vapors to pass and the char mass to stop decreasing. The catalyst bed was post-treated by maintaining its temperature for another 30 min after the biomass pyrolysis reactor was turned off, under hydrogen/nitrogen flow, to allow for any deposited oil/tar to burn off and catalyze further by hydrogenation and deoxygenation. The residence times of the vapors were determined by adjusting the volumetric flow rate exiting the biomass pyrolysis reactor to account for the gas expansions as a result of the temperature changes based on the ideal gas law, using the void volume of the catalyst bed as a constant. Bio char left inside the biomass reactor, and liquid product inside the condenser were collected, quantified and analyzed by GC-MS, KF-titration, and CHN analysis.

*2.4 Gas Chromatography*

The oil phase of the liquid product was extracted using DCM (5:1), of which a 5µL sample was injected into a GC column (Varian Saturn 2200). The column oven was heated to 40°C and held for 6min, ramped to 240°C at 4°C/min and held for 10min, and then again ramped to 280°C at 20°C/min and held for 5 min, for a total time of 73 min [15]. The GC mass spectra peaks were identified using the built in MS library software and the peak areas were integrated to determine the proportional wt. % of each compound in the organic phase. Non-condensable gas samples were collected for composition analysis using GC (SRI 8610C, SRI Instruments) to measure the concentrations of CO, $CO_2$ and $CH_4$. A valuable product, $H_2$ released was not measured due to equipment limitations.

*2.5 KF Titration*

The aqueous content of the liquid product was determined using a KF coulometric titrator (Karl Fischer Titrator Metrohm Model 831 KF Coulometer) (ASTM E203-08). 50µL of the oil sample was mixed with 50mL of ethanol. A 0.5mL sample of the mixture was injected into the coulometer to yield the water content reading in ppm. An ethanol sample was also read to account for any water contributed by the hygroscopic ethanol.

*2.6 Elemental Analysis*

Carbon, Hydrogen and Nitrogen compositions for the biomass, char and oil samples were determined using a 2400 Series 2 CHN (Perkin Elmer, Inc.) elemental analyzer as described in [14]. The oxygen content was determined by taking the difference between 100% and the sum of C, H, and N content.

*2.7 Higher Heating Value*

The HHVs for the oil phases were determined using Dulong's formula [23], where the %CHO values from our elemental analysis were used.

$$HHV \text{ (MJ/kg)} = [338.2*\%C + 1442.8*(\%H-\%O/8)]*0.001 \qquad \text{(Eqn. 1)}$$

For the char solids, the HHV was determined using Demirbas's formula [24],

$$HHV \text{ (MJ/kg)} = 0.3856*(\%C + \%H) - 1.6938 \qquad \text{(Eqn. 2)}$$

*2.8 Statistical Analysis*

A one tail t-test was run wherever mentioned assuming unequal variations, at $\alpha$=0.05. An ANOVA analysis was also run where mentioned, again assuming unequal variations with $\alpha$=0.05. P values less than $\alpha$ were ruled statistically significant between two or more groups of data.

## 3. Results & Discussion

*3.1 Catalyst Analyses*

The temperature-programmed reduction and desorption profiles for the $Pt/Al_2O_3$ catalyst pellets are shown in Figure 2. The profiles show two principal peaks suggesting two different sites with different adsorption strengths. The first reduction peak appeared at around 167˚C, as the platinum oxide is reduced to its metallic form [25]. However, the peak at around 356˚C indicates a class of platinum oxide exhibiting stronger interactions with the support and, hence, requiring higher temperature to reduce [26].

BET analysis on the $Pt/Al_2O_3$ pellets yielded a specific surface area of 100.24 $m^2/g$. The acidity of the catalyst, determined from the peak area of the $NH_3$-TPD profile (Figure 2), was determined to be 1.69 $NH_3$ mmol/g, catalyst.

*3.2 Heating Profiles*

The temperature profiles for the pyrolysis sets heated at different powers using the induction heater, and the one set for the electrical heating tape are shown in Figure 3. In all cases, the temperature rose exponentially to a maximum value as the radiative and convective heat losses began to equal the heat induced. The curves were fitted to a 2-parameter exponential formula after normalizing to 25°C (Table 1).

$$T\,(°C) = a*[1-\exp(-b*t(s))] \qquad \text{(Eqn. 3)}$$

Table 1. Fitting parameters for temperature profiles in each experiment, fitted to an exponential rise to a maximum (2 parameter) formula.

| Experiment | *a* | *b* | *Adj. $R^2$* |
|---|---|---|---|
| *IH 250 W* | 239 | 0.0009 | 0.987 |
| *IH 350 W* | 304 | 0.0008 | 0.990 |
| *IH 500 W* | 386 | 0.0011 | 0.989 |
| *HT 300W* | 220 | 0.0017 | 0.975 |

The maximum steady state temperatures are plotted in Figure 4, which also show the maximum temperature of the ceramic tube loaded with the catalyst pellets only, without steel balls and enveloped within the inductive coil. As it can be observed, high temperatures were unachievable with the catalyst only, without the presence of the steel balls acting as a heating medium. This phenomenon is mostly due to the very weak interaction of the alumina support with the electromagnetic field, as well as due to the high porosity of the catalysts which reduces the overall mass available for electromagnetic interaction and dissipation of energy as heat.

From the temperature profiles it can be deduced that with higher power in the induction heating machine, when steel balls are present, the maximum temperature increased linearly as more current was induced on the surfaces of the balls. The heating rate, given by the parameter *b*, also appears to be faster for the conventional heating method (0.0017) compared

to the inductive heating method (0.0009). This is expected as the temperature controller in the conventional method was operated automatically, whereas the induction heating was controlled manually due to the limitations of the existing equipment.

*3.3 Yields*

The masses of the liquid product and the char left behind were collected and quantified. The difference from the original biomass was taken to determine the mass of gas released for each experiment. With HDO, lower liquid yields and higher gas yields are expected as organic compounds from the decomposition of lignin and cellulose undergo secondary cracking to produce incondensable gases such as CO, $CO_2$ and $CH_4$. Moreover, deoxygenation results in removal of oxygen in the form of CO, $CO_2$ and $H_2O$. Water content also increased as dehydration reactions took place (Figure 5). Both of these effects, the secondary cracking and water production reactions, resulted in a lower oil yield for the catalyzed runs, as is commonly reported in literature for these types of processes and reactions [3, 4, 14, 27]. The complete yield values are listed in Table 2. Lower oil yields were observed for catalyst heated with induction heater compared to heating tape; this is attributed to higher catalyst fouling observed for heating tape (discussed in section 3.6). Higher catalyst fouling implies lower catalyst activity and lower rate of HDO and cracking reactions resulting in higher liquid yields.

Table 2. Yield values (± std. error)

| Sample | Water (wt. %) | Oil (wt. %) | Char (wt. %) | Gas (wt. %) |
|---|---|---|---|---|
| *Baseline* | 18.48 ± 0.31 | 22.52 ± 1.31 | 20.00 ± 0.00 | 39.00 ± 1.00 |
| *HT 237˚C* | 16.59 ± 4.57 | 13.41 ± 3.57 | 21.00 ± 0.00 | 49.00 ± 1.00 |
| *IH 234˚C* | 19.23 ± 1.85 | 6.77 ± 0.85 | 20.00 ± 2.00 | 54.00 ± 1.00 |
| *IH 286˚C* | 17.74 ± 1.45 | 6.76 ± 2.05 | 21.00 ± 1.00 | 54.50 ± 4.50 |
| *IH 375˚C* | 16.09 ± 0.62 | 5.41 ± 2.12 | 23.50 ± 1.50 | 55.00 ± 0.00 |

*3.4 Gas Chromatography*

The GC-MS spectra collected from the oil phase of the liquid products are shown in Figure 6. The peaks were largely identified as phenolic compounds, with traces of alcohols, aldehydes and ketones. Without up-conversion (baseline), the only hydrocarbon identified was that attributed to ethyl benzene. This peak increased in intensity for all up-conversion experiments, but markedly so for the inductive heating experiments. The phenolic peaks, however, were lowest with the induction heating run at 234°C and gradually increased as the temperature of the bed increased. Phenolic compounds generally undergo the HDO reaction to form benzene or cyclohexane after the hydroxyl group is removed via dehydration reactions [4].

However, alkyl ether groups have been reported to negatively influence the reactivity of the phenols while alkyl groups have a positive influence [28]. The peaks shown in Figure 6 show most of the latter removed after upgrading with the induction heater, while the former persist albeit at relatively lower intensities. A summary of the compounds identified were classified as hydrocarbons, phenols, or others (included alcohols, aldehydes and ketones) and are listed for each experiment in Table 3.

Table 3. Summary of organic compounds present in each pyrolysis oil, based on wt. % (± std. error).

| Sample | Hydrocarbons (Wt. %) | Phenols (Wt. %) | Other (Wt. %) |
|---|---|---|---|
| *Baseline* | 7.95 ±2.93 | 66.52 ±2.17 | 25.53 ±1.31 |
| *HT 237˚C* | 13.73 ±1.18 | 61.37 ±0.64 | 24.90 ±0.44 |
| *IH 234˚C* | 29.48 ±0.62 | 39.9 ±0.69 | 30.61 ±0.98 |
| *IH 286˚C* | 25.83 ±1.34 | 47.65 ±2.67 | 26.52 ±3.83 |
| *IH 375˚C* | 33.15 ±0.96 | 48.22 ±7.35 | 18.63 ±3.14 |

Phenolic compounds made up two-thirds of the oil composition before upgrading. For the first catalyzed experiment using the induction heater at the lowest catalyst bed temperature, the composition of phenols decreased to 40 wt.%, while the amount of

hydrocarbons increased from 8 to 30 wt.%. With the presence of the HDO catalyst, partial deoxygenation of the phenols to benzene can be inferred. The other induction heating experiments run at higher bed temperatures gave similar trends for the hydrocarbons, but also showed a gradual increase in phenols with increasing bed temperature.

For the heating tape experiment, a smaller rise in hydrocarbon composition is observed (to 14 wt.%) but the profile is largely identical with respect to the baseline experiment. This suggests that the catalyst surface sites in this experiment were fouled or inhibited relatively fast, preventing the initiation of adsorption of the organic compound. This would imply a large temperature gradient as a result of the slow transfer of heat from the exterior of the tube to the interior. This phenomenon is discussed in more detail in the next sections, where the catalyst surfaces are analyzed post-experiment.

In addition to the GC-MS of the oil phase, GC analysis of the gas product for CO, $CO_2$ and $CH_4$ was performed (Figure 7). Besides HDO, catalytic cracking, which results in the removal of the organic elements from the oil into the gaseous phase, can also take place. The results for the induction heating runs show a slight increasing trend for all the gaseous products as the bed temperature increased, with the exception of the CO under 375°C, which dropped sharply. As the bed temperature increases, the vaporized organic molecules are more likely to undergo additional cracking producing more gaseous products in the form of carbon monoxide, dioxide and smaller-chain hydrocarbons [29]. The large standard error produced for the induction heating 375°C GC test, suggests this data point as a possible outlier. Besides this increasing trend with temperature, there is no discernible pattern of significance for the GC gas analysis.

The absence of a decrease in CO and increase of $CO_2$ as a result of the common oxidation activity for Pt catalyst [30], suggests unfavorable conditions for this particular reaction.

*3.5 Elemental Analysis*

The dry basis C, H and O compositions are listed in Table 4 for the different experiments as well as the biomass and char samples. Using this data we can determine the O/C and H/C molar ratio of the oil samples for the induction-heated and conventionally-heated upgrading experiments and compare them to the oil without deoxygenation (Figure 8). For the experiment run at 234˚C with the induction heater, the O/C molar ratio decreased to 0.51 from 1.36, a 62.5% reduction in the molar oxygen, the highest reduction from all the experiments. The 284˚C experiment had the second highest reduction, down to 0.81, a 40% reduction. The highest bed temperature at 375˚C and the heating tape experiment have almost identical O/C ratios compared to the baseline.

Table 4 Summary of the elemental composition for each pyrolysis run (± std. error)

| Sample | Carbon (Wt. %) | Hydrogen (Wt. %) | Oxygen (Wt. %) |
|---|---|---|---|
| *PSD Biomass* | 49.5 ±1.00 | 6.1 ±0.85 | 44.7 ±0.52 |
| *Char* | 84.4 ±0.69 | 1.8 ±0.08 | 13.5 ±0.72 |
| *Baseline Bio-oil* | 32.3 ±1.61 | 9.5 ±0.66 | 58.2 ±2.28 |
| *Bio-oil HT 237˚C* | 29.2 ±0.08 | 11.0 ±0.01 | 59.8 ±0.08 |
| *Bio-oil IH 234˚C* | 52.8 ±5.32 | 12.7 ±2.35 | 34.5 ±3.02 |
| *Bio-oil IH 286˚C* | 42.9 ±0.82 | 11.0 ±0.01 | 46.1 ±0.82 |
| *Bio-oil IH 375˚C* | 28.5 ±0.67 | 9.4 ±1.59 | 62.1 ±0.92 |

A t-test analysis for each experiment compared to the baseline O/C showed statistical significance for the IH 234 ˚C run only, and no significance for the remaining ones. In addition, no statistical significance between any groups was determined using an ANOVA test for the H/C ratios.

The coke formed in the catalyst was also accounted for by running elemental analysis on the pellets, after single pyrolysis runs with the different heating methods (Figure 9). Clearly, in addition to removing O from the feed, a significant portion of the C is also being removed, leading to an increase in the O/C ratio in the oil. For the case of the heating tape, 26.75% of the total biomass weight was found to be lost in the catalyst bed in the form of coke. If the C from coke is accounted for as shown in Figure 8, the calculated O/C molar ratio would be 0.06. The difference between this value and the reported value of the oil-only value of 1.53 (>96%) for the heating suggests the deoxygenation effect with this method is hampered due to the loss of the C from the oil. In other words, the results from the heating tape and baseline experiment are insignificant from one another, due to the fact that the measured loss of O is offset by the loss of C in the formation of coke. To a lesser extent, this is also seen with the IH 234°C experiment, where an 8.75% loss of C mass was noticed due to the coke formation on the catalyst bed. The O/C ratio calculated included the C from the coke would be 0.047. Data for coke deposition was not collected at the other temperatures.

In addition to losing Carbon over the catalyst bed in the form of coking, elemental mass balances reveal that C and O are also escaping into the gas phase proportionately different compared to the baseline compositions (Figure 10). The higher O/C ratios in the gas phase appear lower at the higher temperatures, which would lead to our observed results, a respective decrease in the O/C ratio of the oil phase at these temperatures.

*3.6 Catalyst fouling and activity analyses*

To understand the discrepancy between the conventional heating and induction heating method for pyrolysis upgrading, the surfaces of the catalysts were examined using $NH_3$-TPD and

BET, and CHN analysis for coke formation. The acidity for the catalysts after a single run using the induction heating method at 234˚C decreased from 1.69 to 1.62$NH_3$ mmol/g, catalyst. Meanwhile, for the heating tape method, the acidic sites decreased from 1.69 to 0.924 $NH_3$ mmol/g, catalyst after a single run (Figure 11), suggesting a fouling of the available acidic sites and hindrance of the adsorption of oxygenated compounds by Lewis-based electron transfer. Oil condensation and coke deposition on the catalyst surface blocks the catalyst pores, decreasing the availability of active reaction sites. Since HDO occurs mainly on the strong acid sites, a decrease in the acid sites due to pore blockage would reduce HDO. The specific BET surface areas revealed a surface area reduction from 100.24 to 95.70 $m^2/g$ for the induction heating method, and to 60.63 $m^2/g$ for the heating tape method, respectively. Again, based on these results it can be deduced that the catalytic active sites are being poisoned under the heating tape at a higher rate than the induction heating method.

While coke deposition hinders the catalyst activity, complete catalytic deactivation was not observed for either of the methods. From TPD analysis, it can be clearly observed that even after coke deposition, some strong acid sites were available for reaction, ensuring reusability of the catalyst. Studies of induction heating for catalyst re-utilization was recently shown to perform well for other catalysts [31], and even though it was not undertaken in this work, based on the TPD data presented it is expected to undergo a similar behavior. Regardless, this is an important issue that will be addressed in detail in a follow-up study.

As it was earlier shown in Figure 9, elemental analysis tested on the catalyst pellets revealed higher C wt. % content for the heating tape experiment after a single run. The rapid poisoning of active sites suggests inability of the catalyst to adsorb the organic molecules to

further deoxygenate and release water, as well as a loss of the carbon content in the catalyst bed. This phenomenon was also deduced from the GC, KF, and CHN analysis performed for the heating tape experiment, where the results resembled closely to those obtained for the pyrolysis oil run without catalytic upgrading. The reason for the better performance of induction heating as opposed to the heating tape can be attributed to direct heating of catalyst bed in the induction system. For the heating tape, due to inefficient heating, the catalyst bed acts as a heat sink while the vapor phase acts as a heat source, driving the product molecules towards the catalyst bed and condensing on the surface. In an induction heater, the metal catalyst is directly heated without the use of heat carrier. This makes the catalyst a heat source rather than a heat sink, reversing the thermal flux and ensuring the movement of product molecules away from the surface reducing deposition and blockage of active sites.

Looking only at the induction heating experiments, a trend appears to show that with increasing temperatures starting from 234°C, the molar O/C increases, and hence the HHV of the oil decreases. In addition, a higher percentage of Carbon was observed to have been lost at the higher temperatures in the gaseous phase. However, one must also look at the interior temperature obtained in the catalyst bed and overlay that information with the TPR and TPD profiles of the catalyst for hydrogen consumption and reactant adsorption. From Figure 11, the two active peaks for reduction and acid site adsorption appear at around 167°C and 356°C.

The bed temperature was calculated for each of the three experiments from the surface tube temperature measured using the IR camera. Using Fourier's heat by conduction law for a multi-layered cylindrical shell (Eqn. 4), the temperature within the tube was estimated, taking into account heat lost due to radiative and convective heat transfer to the surroundings. The

results for the interior temperatures for each experiment are listed in Table 5. For simplification, $T_1$ is taken at half the radial distance from the center to the interior wall, and the bed of steel balls is assumed to be one solid shell. These temperatures are superimposed over the TP profiles in Figure 11 above. The bed temperature at 383°C for IH 375 falls just outside of the second reduction peak, suggesting very little to no hydrogen consumption on the catalyst sites are possible at this temperature.

Table 5. Interior temperatures for the catalyst bed determined using Fourier's Heat by Conduction Law for a 3-layered shell cylinder, and the calculated residence times for each experiment.

$$Q\ (W) = (T_3-T_1)/(R_{Steel}+R_{Tube}) \qquad \text{(Eqn. 4)}$$

| *Experiment* | *Q [W]* | *$T_3$ [°C]* | *$T_1$ [°C]* | *t [s]* |
|---|---|---|---|---|
| *HT 237*°C | 169 | 237 | 232 | 8.46 |
| *IH 234*°C | 122 | 234 | 239 | 8.57 |
| *IH 286*°C | 168 | 286 | 292 | 7.01 |
| *IH 375*°C | 193 | 375 | 383 | 5.34 |

Meanwhile, the experiments run at 292°C and 239°C fall close to the peak of the first reduction and desorption peak. The former showed the second-highest reduction in the O/C ratio, with the loss of more C into the gas phase possibly exacerbating the quality of the oil. At the same time, the lower temperature, which lies closer to the first peak, reflecting the weaker acid sites and reactive metal sites on the catalyst surface, showed the highest deoxygenation effect. The difference between experiments IH 234 and HT 237 (relatively same temperature) underscores the advantage of using induction heating as a heating source for the catalyst bed. Attempting to reach the first peak with the conventional heating method was shown to be problematic as a result of the polycondensation of the bio oil vapors at the low temperature. This is likely due to the cold spots developed as the heat transfers from the walls to the interior

of the bed, and the pellets developing negative temperature gradients across their surfaces. Meanwhile, at the same temperature with the induction heating, partial deoxygenation indicates that moving closer to the first peak is much more possible while avoiding significant condensation, as the heat transfers from the interior of the bed to the walls, and minimizing the temperature gradients across the surface.

Another factor to consider is the contact time of the reactants with the catalyst sites. The residence times for each experiment are also listed in Table 5, with the expansion of the gas with temperature increases taken into account using the ideal gas law. With higher temperatures, the catalyst contact time decreased significantly which suggests less time for HDO to take place. A recommendation for future work would be to increase the length of the tube, as well as the coil, for longer residence times.

*3.7 Energy Balances*

The HHVs of the oil phases for each experiment are listed in Table 6. As shown, the HHV value of the bio-oil upgraded at the lowest induction heated catalyst bed, 28.82MJ/kg, is almost twice the value obtained for the heating tape experiment (15.00MJ/kg), which is almost identical to the HHV of the oil without up-conversion (14.12MJ/kg).

Table 6. Energy Balances (with std. errors)

| *Experiment* | Higher Heating Value of the oil (MJ/kg) | Input Energy -process equipment, biomass (kJ) | Output Energy -char, oil, gas (kJ) | Net Loss (kJ) | Biomass Energy Recovered (%) |
|---|---|---|---|---|---|
| *CONTROL* | 14.12 ±1.91 | 1466 ±7.14 | 105 ±4.50 | 1361 ±5.97 | 53.2 ±0.36 |
| *HT 237˚C* | 15.00 ± 0.04 | 1826 ±7.14 | 88 ±0.14 | 1738 ±5.05 | 44.6 ±1.69 |
| *IH 234˚C* | 28.82 ±0.55 | 1766 ±7.14 | 105 ±3.55 | 1661 ±5.64 | 53.3 ±0.13 |
| *IH 286˚C* | 22.81 ±0.16 | 1886 ±7.14 | 108 ±4.21 | 1779 ±5.86 | 54.7 ±0.15 |
| *IH 375˚C* | 12.06 ±2.23 | 2066 ±7.14 | 110 ±2.87 | 1956 ±5.44 | 56.0 ±0.57 |

The energy inputs and outputs for each pyrolysis experiment over the duration of the run (20min) are also listed in Table 6, with the net loss listed in the third column. The input energy included the operational equipment running during the pyrolysis such as the induction heater, ESP, as well as the calorific values of the biomass and hydrogen gas flowing in. The values in the energy output were the derived calorific values of the char, oil and gas products. Being unable to measure the hydrogen exiting the system as well as other low molecular weight hydrocarbons ($C_2$-$C_5$) [14], our net losses may appear larger than actual losses.

The determined net loss appeared higher for the heating tape experiment compared to its similar induction heating counterpart. This is a result of the minimal-to-no deoxygenation achieved in the heating tape experiment, compared to the induction heating. The induction heating experiments at higher bed temperatures (286˚C and 375˚C) predictably showed much higher net losses as a result of the necessary additional power to maintain the higher temperatures, with little additional upgrading of the oil to contribute toward a higher HHV.

The energy values recovered in our products from the original biomass are listed for each experiment. All tests revealed roughly equal recovery amounts, except for the heating tape experiment which had the highest loss of C in the catalyst bed. While the energy recovered is identical for the both the upgraded and non-upgraded experiments, mainly due to the loss of the oil yield in the former, it is important to note that the energy is distributed among fewer molecules as shown in our GC-MS spectra earlier compared to the baseline. This indicates the upgraded product is more homogenous, stable and extractable comparatively. Raw bio-oil contains hundreds, even thousands, of organic compounds, making the process of separating and collecting the desired compounds arduous and costly [32]. It also increases the

reactivity within the oil makeup as these mostly oxygenated compounds interact with each other and alter the chemical composition of the oil. This 'aging' of the oil not only deteriorates the quality of the oil, but also complicates the chemical extraction process [31, 32]. By reducing the chemical makeup of the oil to a handful of compounds and concentrating the energy density, separation costs are reduced and spontaneous reactions are less likely to take place.

To mitigate the energy losses in our process, the use of insulation on the both the biomass and catalyst bed tubes would assist in the reduction of the amount of power needed to maintain both reactor temperatures, by minimizing radiative and convective heat losses The insulation could not be used in these studies due to the operation of the upgrading equipment at very low power levels (3-5%), very close to the minimum possible for stable operations (the equipment is not designed to operate at 1-2% of the maximum power). Thus, the equipment was operated in an energy inefficient manner in order to prevent equipment malfunction, as additional insulation would drop the power requirements below this limit.

In addition, scaling up both the biomass and catalyst amounts will help reduce the net loss by increasing our output-to-input energy. The reactor sizes would remain identical, as they were not optimized in this experiment, and the larger biomass and catalyst pellet loadings will increase the effect of HDO, and improve the energy recovery of the upconversion process.

## 4. Conclusion

Using induction heating as a source for a steel-packed catalyst bed, up-conversion of sawdust pyrolysis oil was achieved by partial deoxygenation with $Pt/Al_2O_3$. The optimal temperature of the bed needed for hydrogen reduction was determined to be around 230-240°C. A conventional heating method, using an electric heating tape as an external heat source

was used as a control. In this control experiment, heating the bed to the same optimal temperature (as observed in induction heating) resulted in rapid fouling of the catalyst via coke formation with little-to-no deoxygenation. The study described in this paper helps support induction heating as a lucrative heating source for a catalyst bed coupled with conductive material to aid in driving the temperature gradient from the interior to the exterior of the tube, and avoiding heat transfer loss. This opens the door to looking at catalytic supports with high electrical conductivity to increase the lifetime of the catalyst by heating the pellets directly and preventing the deposition of coke and other pollutants.

**Acknowledgements**

This work was funded by the National Science Foundation (NSF) (#CBET 1437810). Partial support was also provided by the LSU AgCenter, the Department of Biological and Agricultural Engineering at LSU, USDA NIFA via Hatch Program (project LAB #94196), Louisiana Board of Regents Enhancement Program (award # LEQSF(2015-17)-ENH-TR-01), and Louisiana Transportation Research Center (proposal #40201). The authors would like to thank Dr. James Spivey, Zi Wang, Dr. Nitin Kumar, Dr. Tommy Blanchard, Dr. Charlie Milan, Connie David, Gustavo Aguilar and Charles Henkel for their technical assistance during these studies. The manuscript was published with the approval of the Director of the Louisiana Agricultural Experiment Station as manuscript # 2016-232-27532.

**References**

[1] T. Dickerson, J. Soria, Energ., 6 (2013) 514-538.
[2] P.M. Mortensen, J.-D. Grunwaldt, P.A. Jensen, K. Knudsen, A.D. Jensen, Appl. Catal. A: Gen., 407 (2011) 1-19.
[3] J. Payormhorm, K. Kangvansaichol, P. Reubroycharoen, P. Kuchonthara, N. Hinchiranan, Bioresour. Technol., 139 (2013) 128-135.
[4] M. Zanuttini, C. Lago, C. Querini, M. Peralta, Catal. Today, 213 (2013) 9-17.

[5] A. Oasmaa, S. Czernik, Energ. Fuels, 13 (1999) 914-921.
[6] Q. Zhang, J. Chang, T. Wang, Y. Xu, Energ. Convers. Manag., 48 (2007) 87-92.
[7] R. Venderbosch, A. Ardiyanti, J. Wildschut, A. Oasmaa, H. Heeres, J. Chem.Technol. Biotechnol., 85 (2010) 674-686.
[8] V.N. Bui, D. Laurenti, P. Afanasiev, C. Geantet, Appl. Catal. B- Environ., 101 (2011) 239-245.
[9] R. Kallury, T. Tidwell, D. Boocock, D. Chow, Can. J. of Chem., 62 (1984) 2540-2545.
[10] C.R. Lee, J.S. Yoon, Y.-W. Suh, J.-W. Choi, J.-M. Ha, D.J. Suh, Y.-K. Park, Catal. Commun., 17 (2012) 54-58.
[11] E.O. Odebunmi, D.F. Ollis, J. of Catal., 80 (1983) 56-64.
[12] Y. Romero, F. Richard, Y. Ren me, S. Brunet, Appl. Catal. A: Gen., 353 (2009) 46-53.
[13] W. Wang, Y. Yang, H. Luo, T. Hu, W. Liu, Catal. Commun., 12 (2011) 436-440.
[14] C. Henkel, P.D. Muley, K.K. Abdollahi, C. Marculescu, D. Boldor, Energ. Convers. Manag., 109 (2016) 175-183.
[15] P.D. Muley, C. Henkel, K.K. Abdollahi, D. Boldor, Energ. Fuels, 29 (2015) 7375-7385.
[16] W. Moreland, IEEE Trans. on Ind. Applicat., 1 (1973) 81-85.
[17] J. Akhtar, N.S. Amin, Renew. Sustain. Energ. Rev., 16 (2012) 5101-5109.
[18] D.M. Bibby, R.F. Howe, G.D. McLellan, Appl. Catal. A: Gen., 93 (1992) 1-34.
[19] C.M. Schietekat, S.A. Sarris, P.A. Reyniers, L.B. Kool, W. Peng, P. Lucas, K.M. Van Geem, G.B. Marin, Ind. Eng. Chem. Res., 54 (2015) 9525-9535.
[20] B. Zhang, Z. Zhong, Q. Xie, P. Chen, R. Ruan, RSC Adv., 5 (2015) 56286-56292.
[21] Z. Wang, J.J. Spivey, Appl. Catal. A: Gen., 507 (2015) 75-81.
[22] M.M. Abu-Laban, Biomass Catalytic Upconversion with a Metallic Catalyst Bed under Radio Frequency Induction Heating, M.S Thesis. Biological and Agricultural Engineering, Louisiana State University, Baton Rouge, LA, USA, 2016.
[23] S. Channiwala, P. Parikh, Fuel, 81 (2002) 1051-1063.
[24] A. Demirbaş, Fuel, 76 (1997) 431-434.
[25] E.-Y. Ko, E.D. Park, K.W. Seo, H.C. Lee, D. Lee, S. Kim, Catal. Lett., 110 (2006) 275-279.
[26] F. Pompeo, G. Santori, N.N. Nichio, Int. J. of Hydrog. Energ., 35 (2010) 8912-8920.
[27] C.A. Fisk, T. Morgan, Y. Ji, M. Crocker, C. Crofcheck, S.A. Lewis, Appl. Catal. A: Gen., 358 (2009) 150-156.
[28] E. Furimsky, Appl. Catal. A: Gen., 199 (2000) 147-190.
[29] M.I. Jahirul, M.G. Rasul, A.A. Chowdhury, N. Ashwath, Energ., 5 (2012) 4952-5001.
[30] A.D. Allian, K. Takanabe, K.L. Fujdala, X. Hao, T.J. Truex, J. Cai, C. Buda, M. Neurock, E. Iglesia, J. of the Am. Chem. Soc., 133 (2011) 4498-4517.
[31] P. Muley, C. Henkel, G. Aguilar, K. Klasson, D. Boldor, Applied Energy, 183 (2016) 995-1004.
[32] D. Chen, J. Zhou, Q. Zhang, X. Zhu, Renew. Sustain. Energ. Rev., 40 (2014) 69-79.

**Figure 1. IR Image**. Thermal image recorded by the user interface of the ThermaCAM Professional 9.1 data acquisition software (left), used to measure infrared radiation of heated surfaces, compared to image of actual catalyst bed enveloped in coil (right).

**Figure 2. TPD & TPR Profiles**. Temperature-programmed reduction with $H_2$ and temperature-programmed desorption with $NH_3$ profiles for the Pt (1 wt.%)/$Al_2O_3$ pellets.

**Figure 3. Heating Profiles**. Temperature plots recorded using IR camera and ThermaCam data acquisition for catalyst bed heated under RF inductive field at 3 different powers: 250W, 350W, and 500W, and with electrical heating tape (HT 300W).

**Figure 4. Steady-State Temperatures**. Maximum steady state temperature are plotted for the catalyst bed with no steel balls, the bed mixed with steel balls and heated at 3 different power levels, and the bed heated with electrical heating tape.

**Figure 5. Water & Bio-oil Yields**. Water and oil composition of pyrolysis liquid product, determined using KF titration.

**Figure 6. Gas Chromatography Mass Spectrometry.** GC-MS spectra for the inductive and conventional heating samples, at 234˚C and 237˚C respectively, compared to the non-upgraded oil sample.

**Figure 7. CO, $CO_2$, $CH_4$ Quantification**. GC-Gas analysis of the gas samples collected during pyrolysis for carbon monoxide, dioxide and methane quantification.

**Figure 8. Molar O:C, H:C**. Oxygen-to-carbon, and hydrogen-to-carbon molar ratios for the control and upgraded samples based on their elemental analyses. For the two heating comparison experiments (234/237˚C), the ratios accounting for the coke deposited on catalyst is also displayed to underscore effect of the deposition on the overall O/C content of the oil between the two methods.

**Figure 9. Coke Content**. C elemental analysis on the Pt/$Al_2O_3$ pellets after single pyrolysis upgrading runs for the two heating comparison experiments, reflecting coke deposition quantity.

**Figure 10. Elemental Mass Balances**. C (a), O (b), and H (c) wt.% balances over the respective products formed.

**Figure 11. TPD & TPR Profiles**. $NH_3$-TPD profiles for fresh catalysts (control) compared to inductively-heated (IH234˚C) and conventionally-heated (HT 237˚C) catalysts after single run pyrolysis up-conversion.

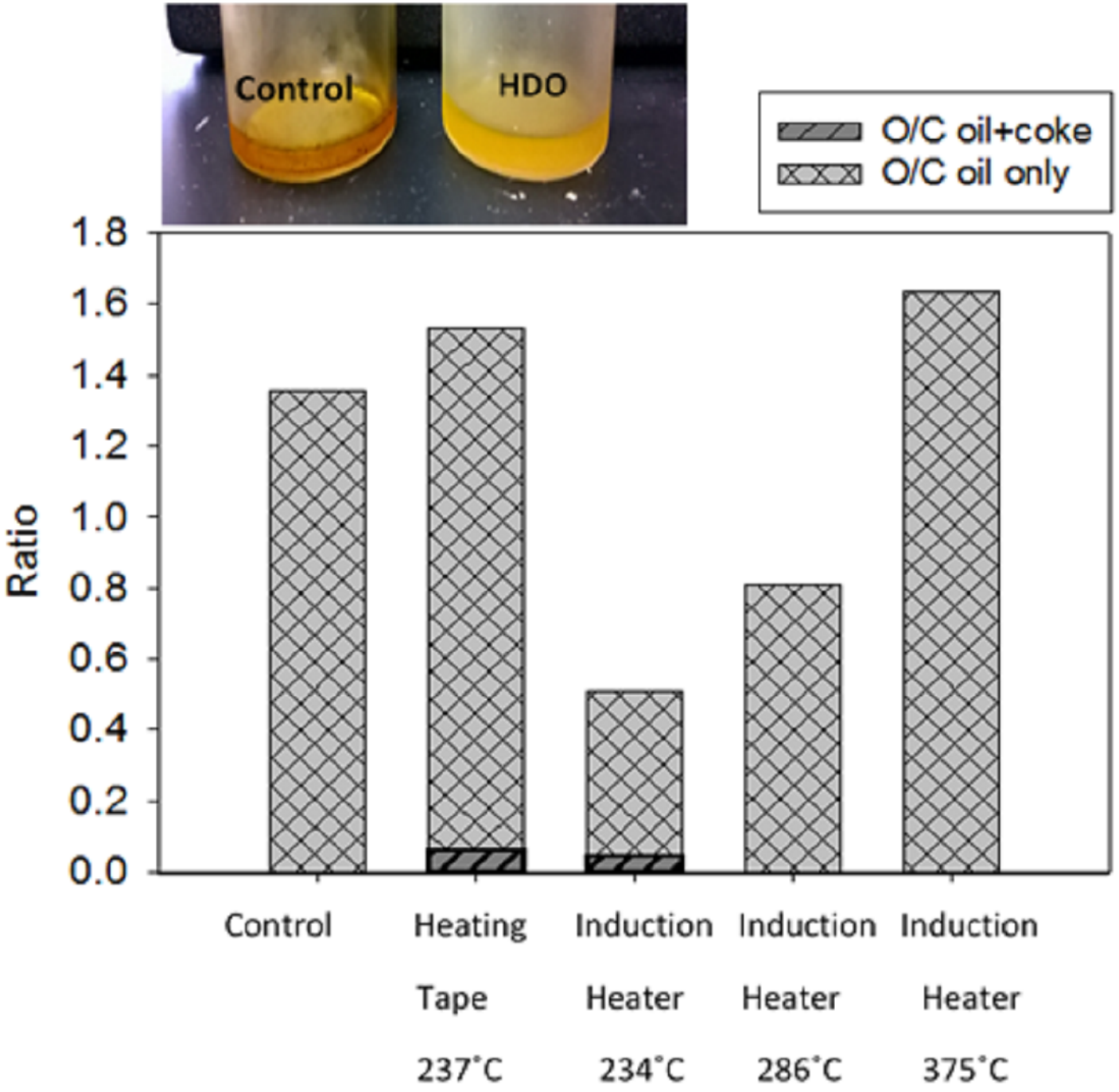
Control
HDO
O/C oil+coke
O/C oil only
Ratio
1.8
1.6
1.4
1.2
1.0
0.8
0.6
0.4
0.2
0.0
Control
Heating Tape 237˚C
Induction Heater 234˚C
Induction Heater 286˚C
Induction Heater 375˚C

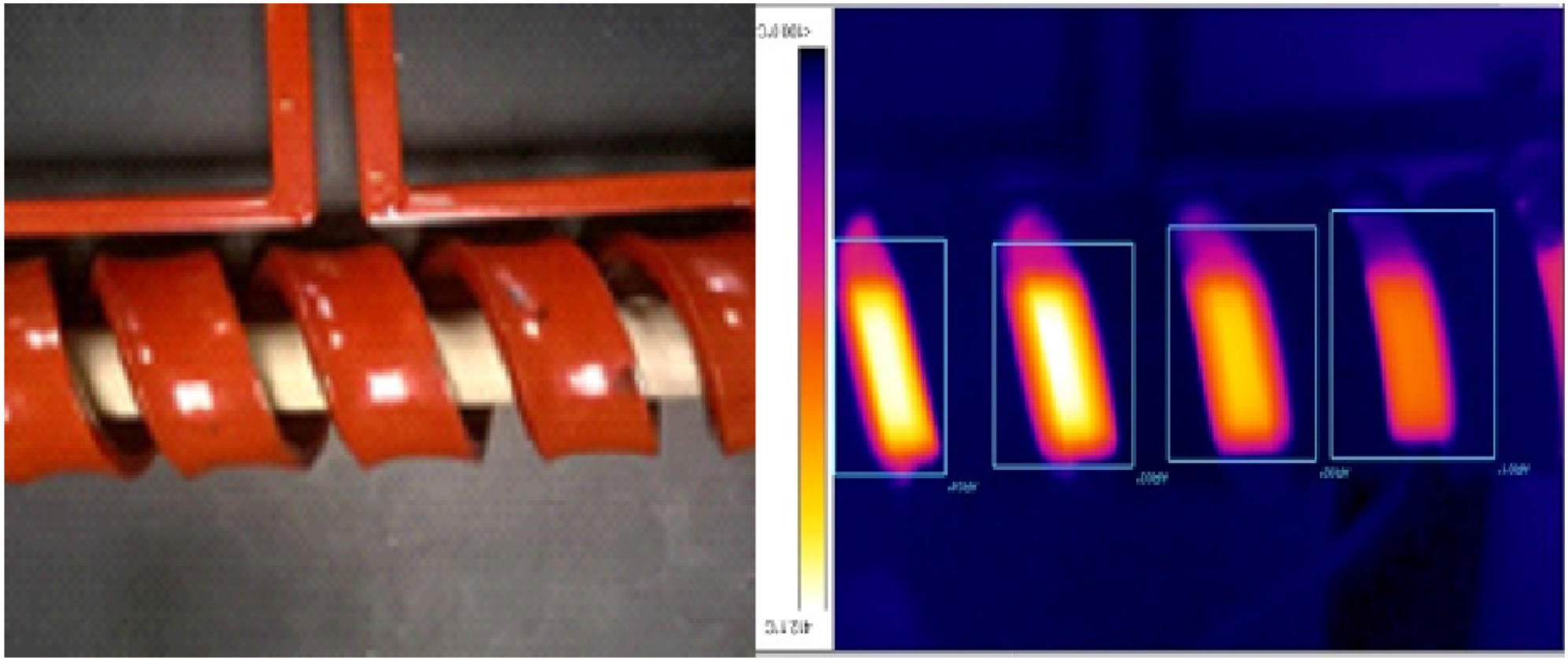

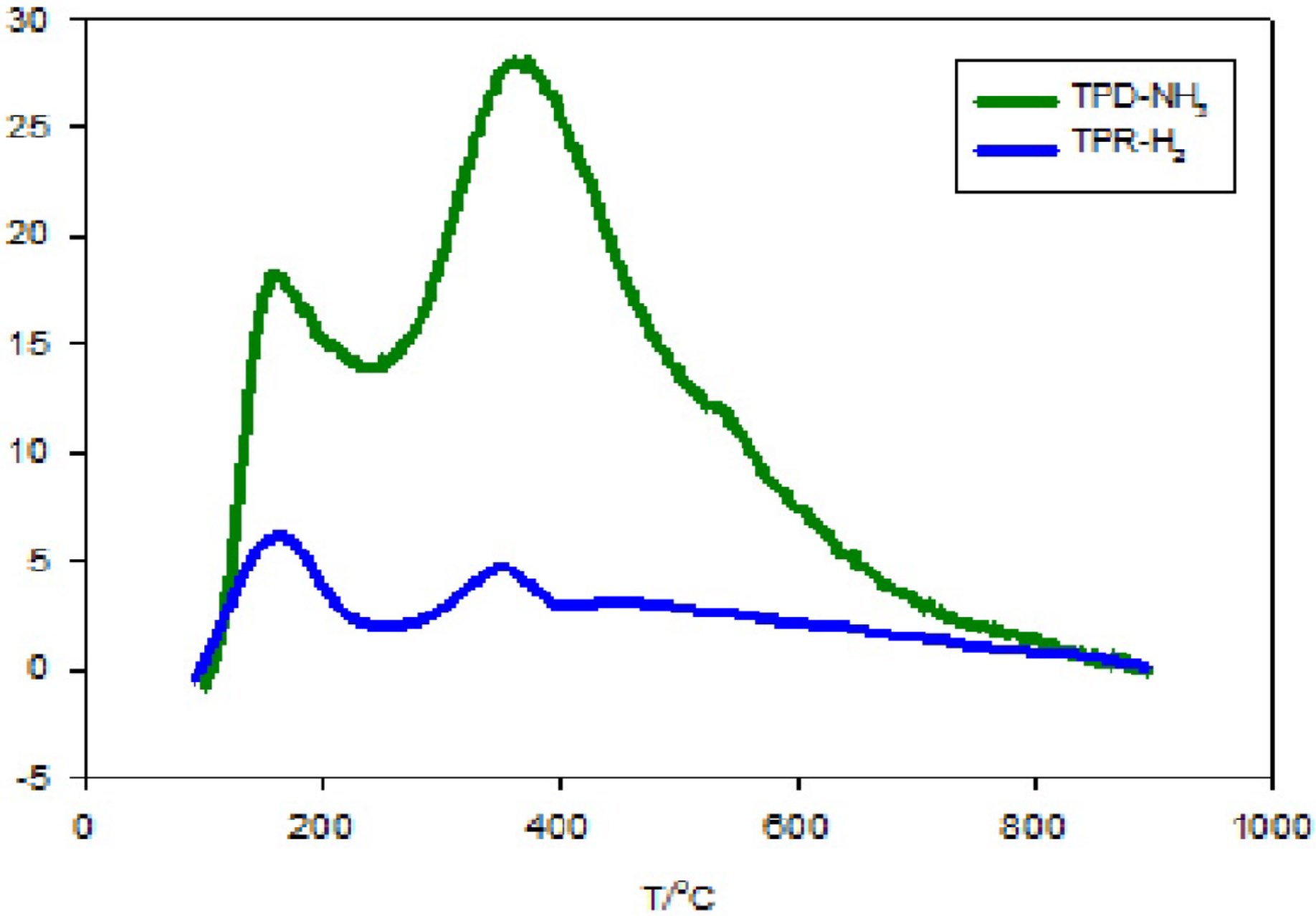
30
25
20
15
10
5
0
-5
0
200
400
600
800
1000
T/°C
TPD-NH3
TPR-H2

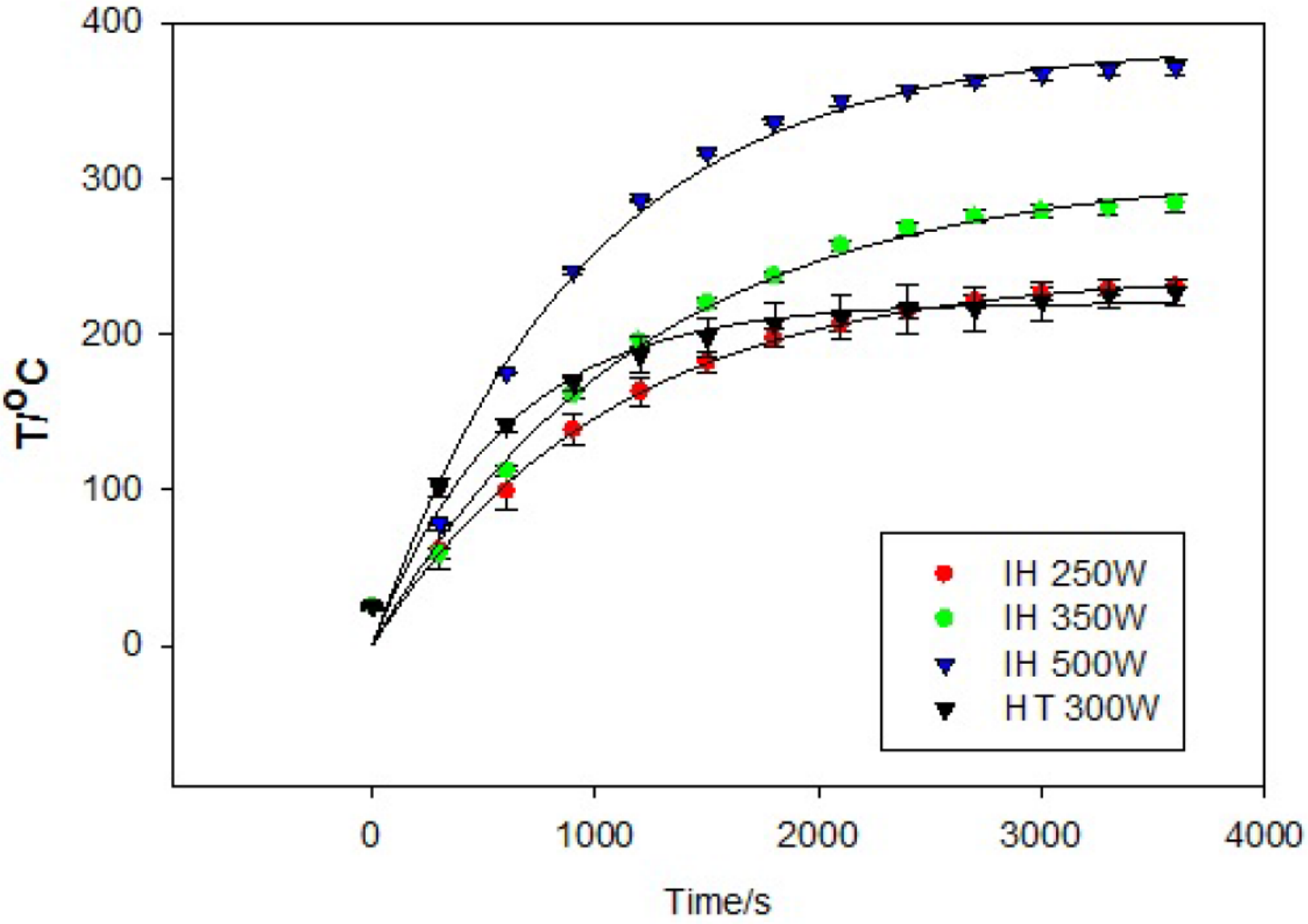
400
300
200
100
0
T/°C
0
1000
2000
3000
4000
Time/s
IH 250W
IH 350W
IH 500W
HT 300W

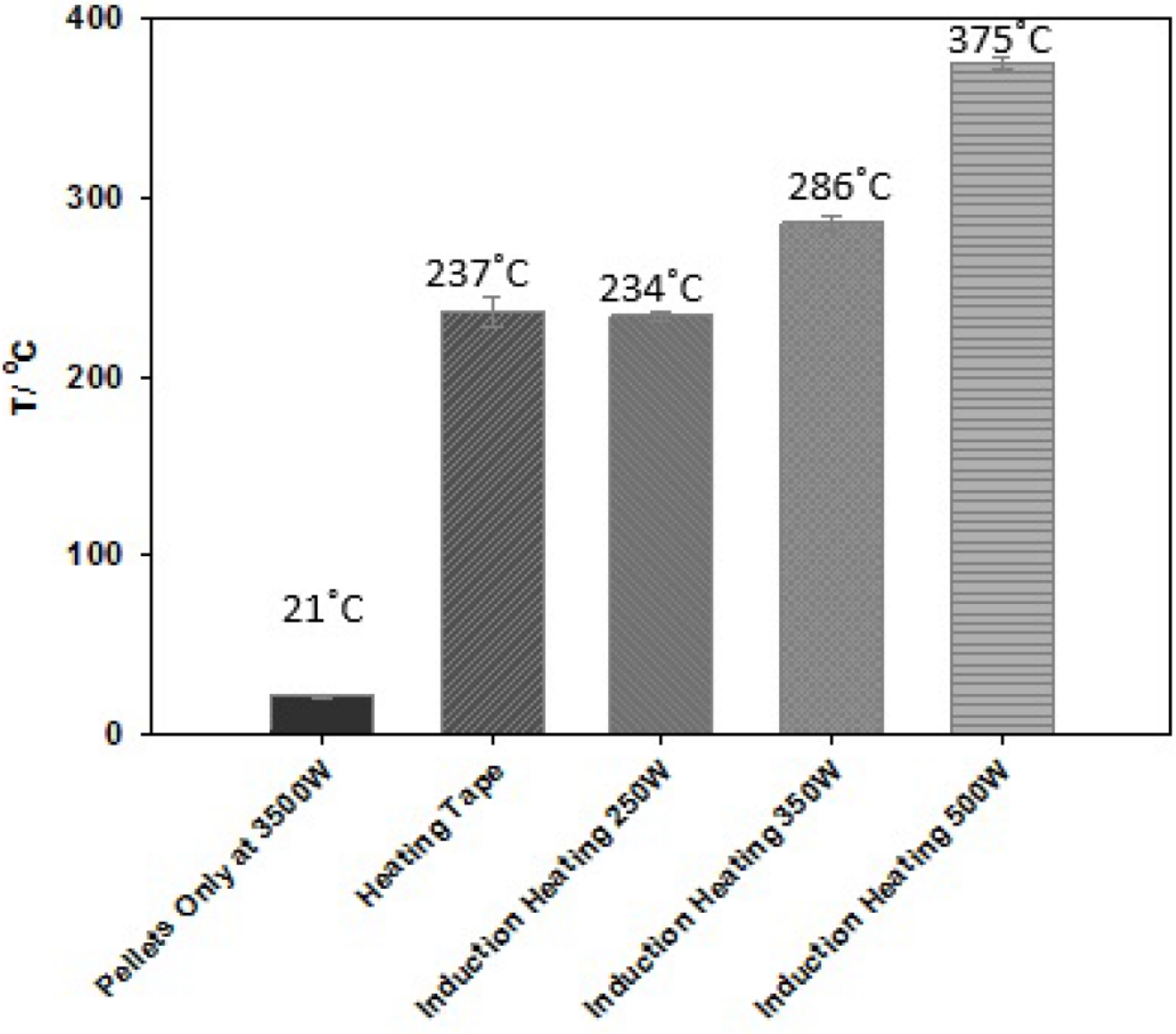
400
300
200
100
0
T/ °C
21˚C
237˚C
234˚C
286˚C
375˚C
Pellets Only at 3500W
Heating Tape
Induction Heating 250W
Induction Heating 350W
Induction Heating 500W

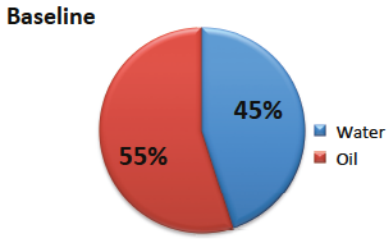
Baseline
45%
55%
Water
Oil

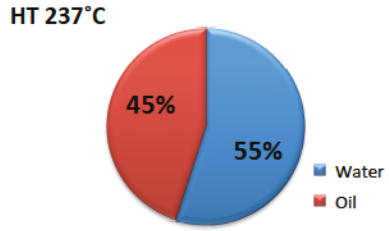
HT 237˚C
45%
55%
Water
Oil

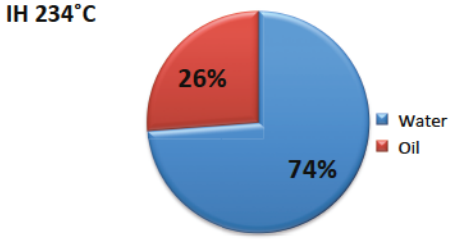
IH 234˚C
26%
74%
Water
Oil

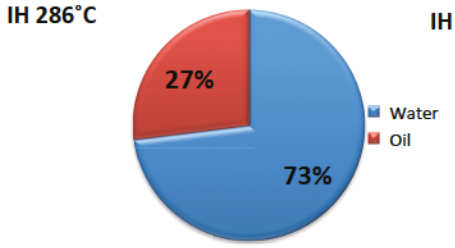
IH 286˚C
27%
73%
Water
Oil

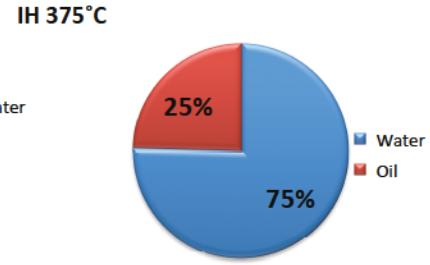
IH 375˚C
25%
75%
Water
Oil

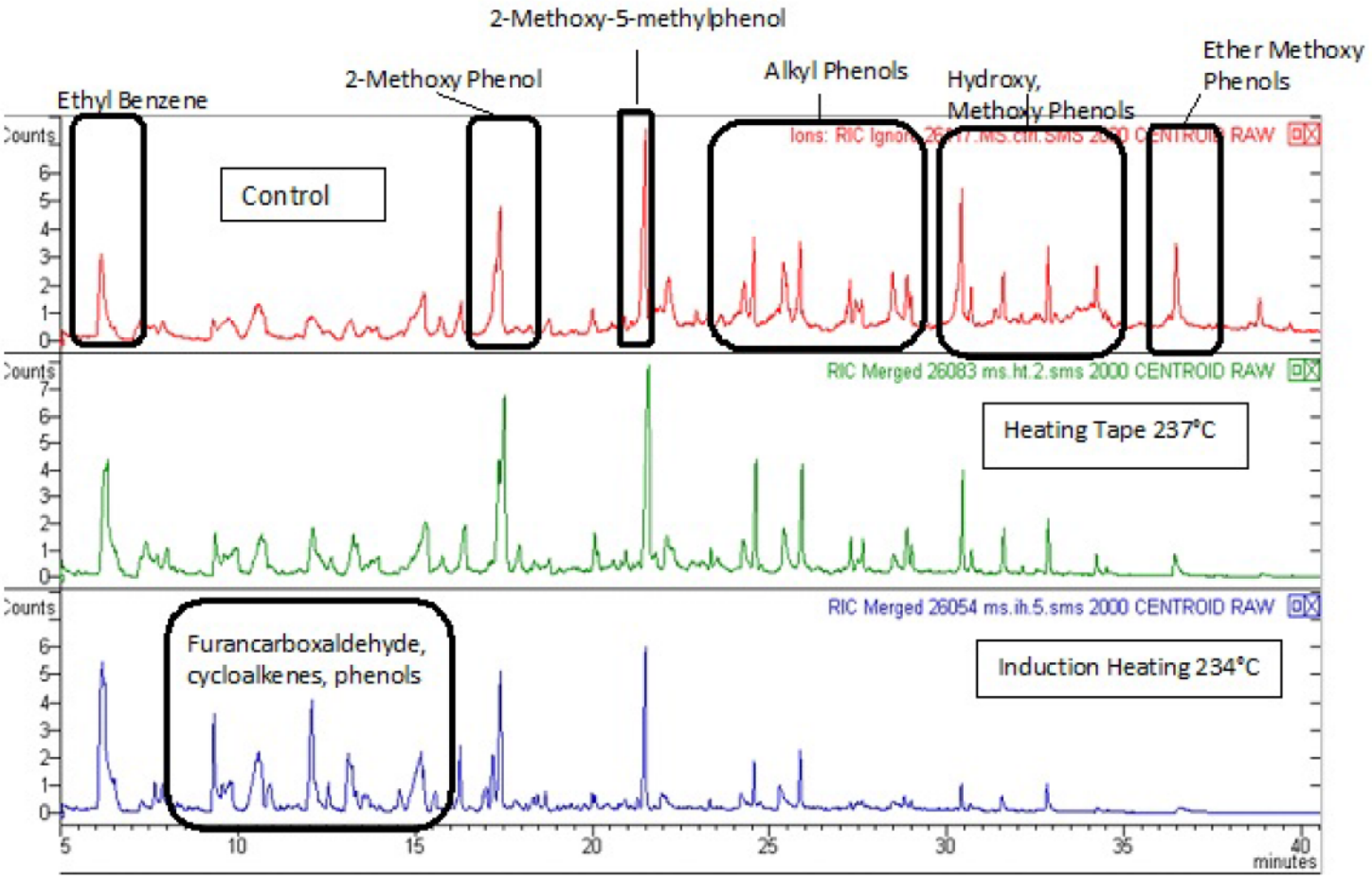
2-Methoxy-5-methylphenol
Ether Methoxy Phenols
2-Methoxy Phenol
Alkyl Phenols
Hydroxy, Methoxy Phenols
Ethyl Benzene
Control
Heating Tape 237°C
Induction Heating 234°C
Furancarboxaldehyde, cycloalkenes, phenols
minutes

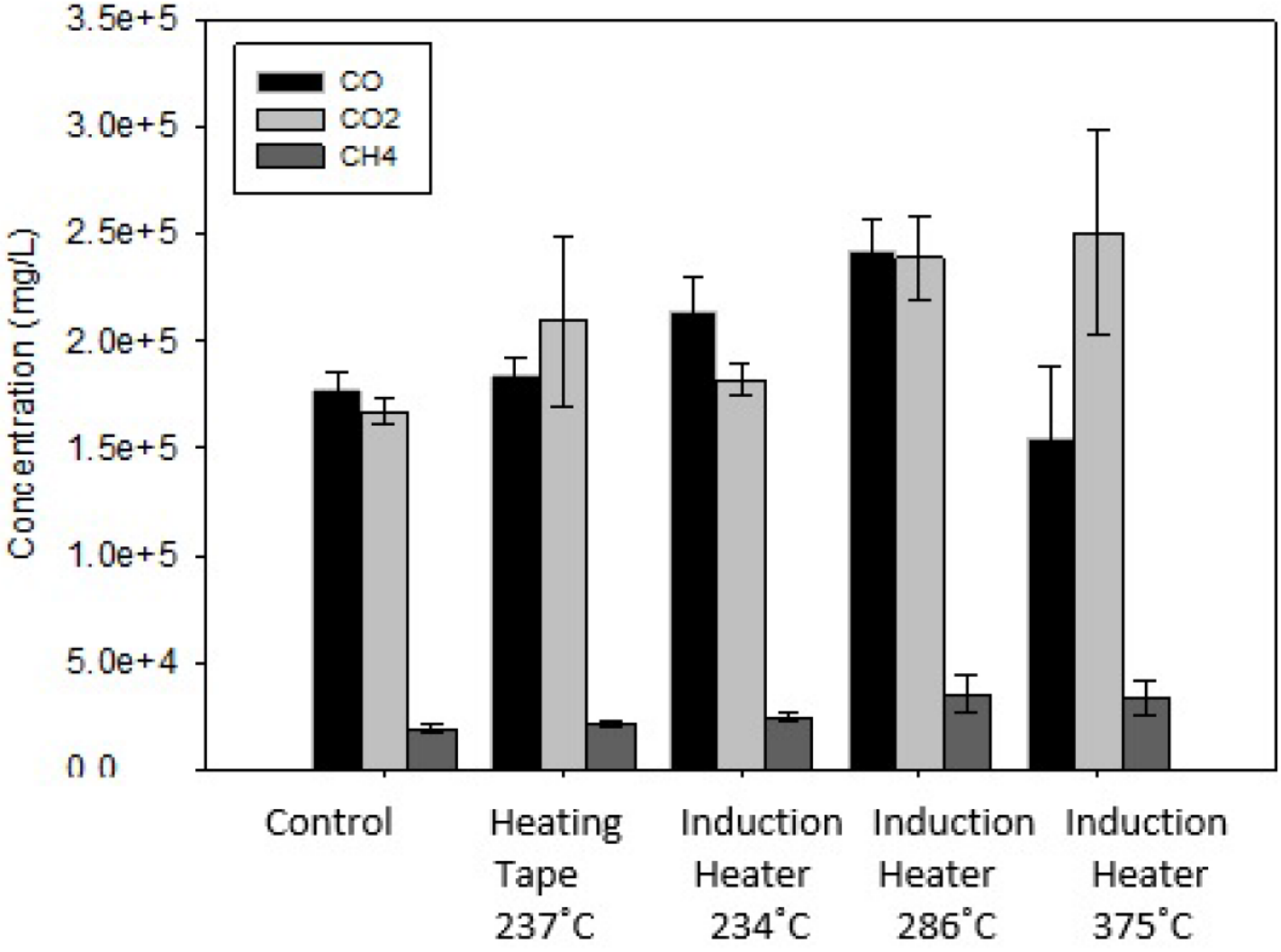
3.5e+5
3.0e+5
2.5e+5
2.0e+5
1.5e+5
1.0e+5
5.0e+4
0.0
Concentration (mg/L)
CO
CO2
CH4
Control
Heating Tape 237˚C
Induction Heater 234˚C
Induction Heater 286˚C
Induction Heater 375˚C

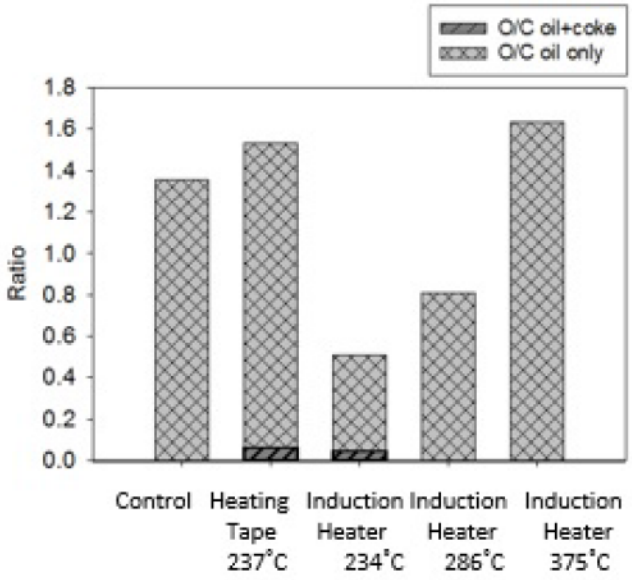
O/C oil+coke
O/C oil only
Ratio
1.8
1.6
1.4
1.2
1.0
0.8
0.6
0.4
0.2
0.0
Control
Heating Tape 237˚C
Induction Heater 234˚C
Induction Heater 286˚C
Induction Heater 375˚C

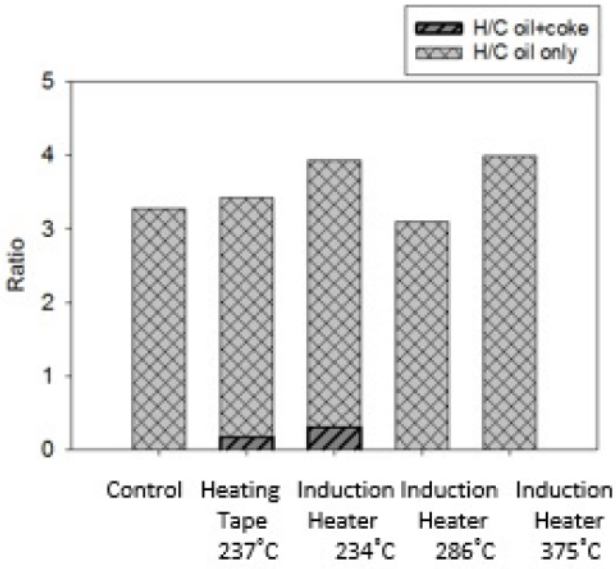
H/C oil+coke
H/C oil only
Ratio
5
4
3
2
1
0
Control
Heating Tape 237˚C
Induction Heater 234˚C
Induction Heater 286˚C
Induction Heater 375˚C

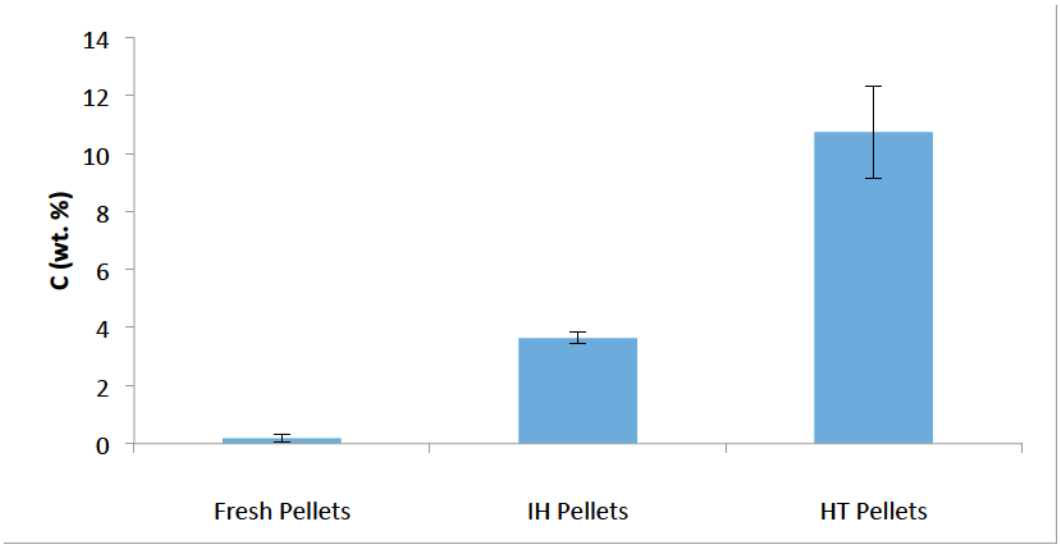
14
12
10
8
6
4
2
0
C (wt. %)
Fresh Pellets
IH Pellets
HT Pellets

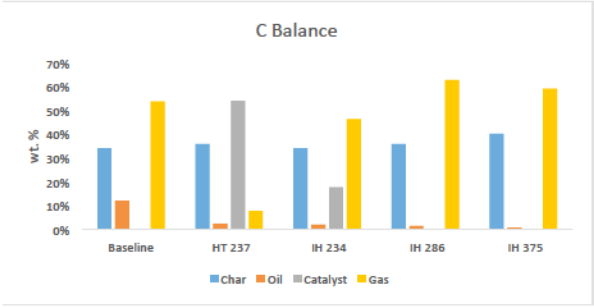
C Balance
wt. %
70%
60%
50%
40%
30%
20%
10%
0%
Baseline
HT 237
IH 234
IH 286
IH 375
Char
Oil
Catalyst
Gas

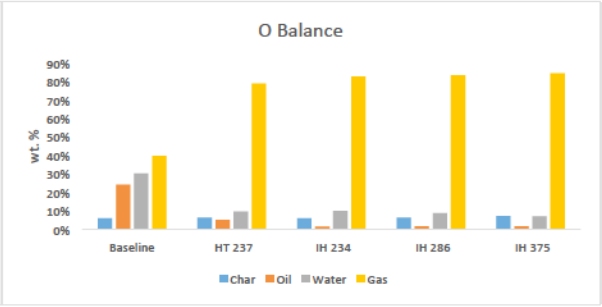
O Balance
wt. %
90%
80%
70%
60%
50%
40%
30%
20%
10%
0%
Baseline
HT 237
IH 234
IH 286
IH 375
Char
Oil
Water
Gas

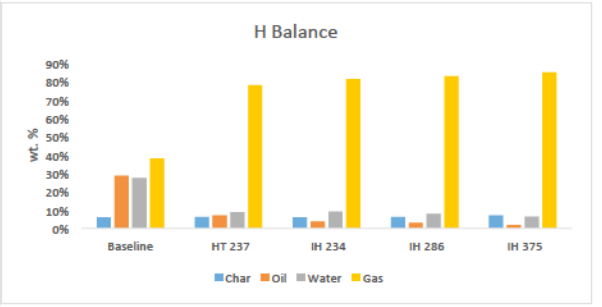
H Balance
wt. %
90%
80%
70%
60%
50%
40%
30%
20%
10%
0%
Baseline
HT 237
IH 234
IH 286
IH 375
Char
Oil
Water
Gas

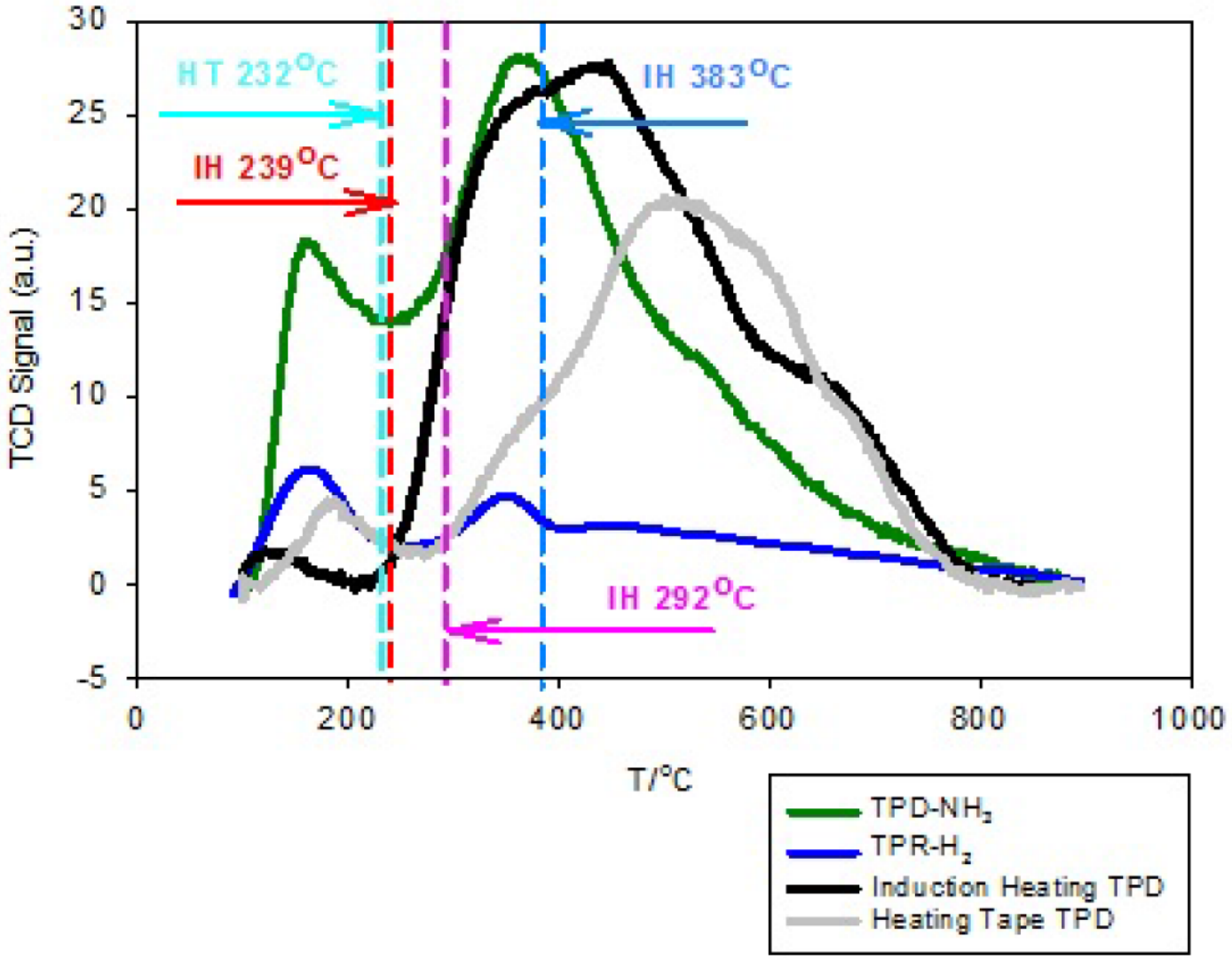
HT 232°C
IH 239°C
IH 383°C
IH 292°C
TCD Signal (a.u.)
T/°C
30
25
20
15
10
5
0
-5
0
200
400
600
800
1000
TPD-NH3
TPR-H2
Induction Heating TPD
Heating Tape TPD

**Supplemental Information**

# Ex-situ up-conversion of biomass pyrolysis bio-oil vapors using $Pt/Al_2O_3$ nanostructured catalyst synergistically heated with steel balls via induction

Mohammad Abu-Laban[1], Pranjali D. Muley[1],Daniel J. Hayes[1], and Dorin Boldor[1,*]

[1]Department of Biological & Agricultural Engineering, Louisiana State University Agricultural Center and A&M College, Baton Rouge, Louisiana 70803, United States of America

[*]Corresponding author. Email address: dboldor@agcenter.lsu.edu

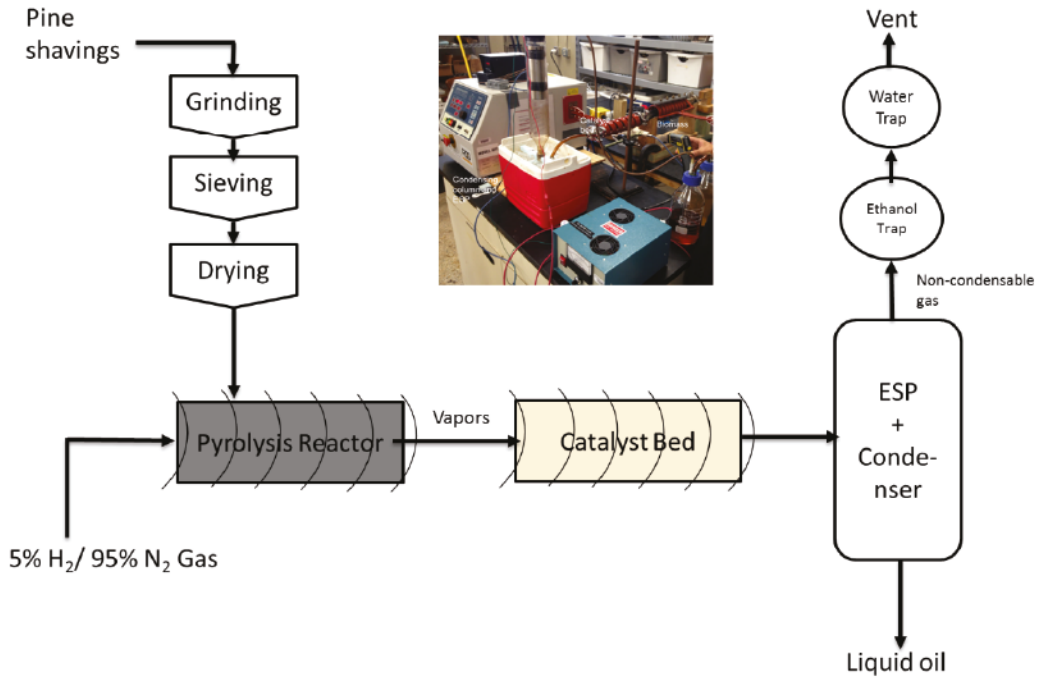


**Figure 1**. Experimental setup of pyrolysis upconversion experiment. Pretreated biomass is loaded into cylindrical tube and purged with diluted hydrogen gas. Gases pass through sequentially into catalyst bed reactor followed by condenser, where oil collection occurs, and vent.

| **O:C Statistical Analyses** | | |
|---|---|---|
| t-Test: Two-Sample Assuming Unequal Variances | | |
| | | |
| | *Control* | *Heating Tape* |
| Mean | 1.35729673 | 1.53513545 |
| Variance | 0.02912069 | 7.2675E-05 |
| Observations | 2 | 2 |
| Hypothesized Mean Difference | 0 | |
| df | 1 | |
| t Stat | -1.4719709 | |
| P(T<=t) one-tail | 0.18994816 | |
| t Critical one-tail | 6.31375151 | |
| P(T<=t) two-tail | 0.37989632 | |
| t Critical two-tail | 12.7062047 | |
| | | |
| | | |
| t-Test: Two-Sample Assuming Unequal Variances | | |
| | | |
| | *Control* | *IH 250* |
| Mean | 1.35729673 | 0.50723139 |
| Variance | 0.02912069 | 0.0229736 |
| Observations | 2 | 3 |
| Hypothesized Mean Difference | 0 | |
| df | 2 | |
| t Stat | 5.70292622 | |
| P(T<=t) one-tail | 0.014699 | |
| t Critical one-tail | 2.91998558 | |
| P(T<=t) two-tail | 0.02939801 | |
| t Critical two-tail | 4.30265273 | |
| | | |
| | | |
| t-Test: Two-Sample Assuming Unequal Variances | | |
| | | |
| | *Control* | *IH 350* |
| Mean | 1.35729673 | 0.80908282 |
| Variance | 0.02912069 | 0.00358496 |
| Observations | 2 | 4 |
| Hypothesized Mean Difference | 0 | |
| df | 1 | |
| t Stat | 4.40953979 | |
| P(T<=t) one-tail | 0.07098597 | |
| t Critical one-tail | 6.31375151 | |
| P(T<=t) two-tail | 0.14197194 | |
| t Critical two-tail | 12.7062047 | |
| | | |

| | | |
|---|---|---|
| t-Test: Two-Sample Assuming Unequal Variances | | |
| | | |
| | *Control* | *IH 500* |
| Mean | 1.35729673 | 1.63319773 |
| Variance | 0.02912069 | 0.00040361 |
| Observations | 2 | 2 |
| Hypothesized Mean Difference | 0 | |
| df | 1 | |
| t Stat | -2.2707977 | |
| P(T<=t) one-tail | 0.13204133 | |
| t Critical one-tail | 6.31375151 | |
| P(T<=t) two-tail | 0.26408266 | |
| t Critical two-tail | 12.7062047 | |

| **H:C Statistical Analyses** | | | | | | |
|---|---|---|---|---|---|---|
| Control | 3.00934892 | 3.02022021 | 3.45201643 | 3.59269121 | | |
| HT | 2.36897293 | 2.25266747 | 4.54246321 | 4.5185608 | | |
| IH 234 | 4.35963362 | 4.26785352 | 3.16363552 | | | |
| IH 286 | 3.01039718 | 2.96824713 | 3.19225266 | 3.19326012 | | |
| IH 375 | 4.75309489 | 3.22692491 | | | | |
| | | | | | | |
| | | | | | | |
| Anova: Single Factor | | | | | | |
| | | | | | | |
| SUMMARY | | | | | | |
| *Groups* | *Count* | *Sum* | *Average* | *Variance* | | |
| Control | 4 | 13.0742768 | 3.26856919 | 0.08919345 | | |
| HT | 4 | 13.6826644 | 3.4206661 | 1.64469362 | | |
| IH 234 | 3 | 11.7911227 | 3.93037422 | 0.44302207 | | |
| IH 286 | 4 | 12.3641571 | 3.09103927 | 0.01409144 | | |
| IH 375 | 2 | 7.9800198 | 3.9900099 | 1.16459739 | | |
| | | | | | | |
| | | | | | | |
| ANOVA | | | | | | |
| *Source of Variation* | *SS* | *df* | *MS* | *F* | *P-value* | *F crit* |
| Between Groups | 1.92256943 | 4 | 0.48064236 | 0.7906844 | 0.5532189 | 3.25916673 |
| Within Groups | 7.29457704 | 12 | 0.60788142 | | | |
| | | | | | | |
| Total | 9.21714647 | 16 | | | | |